BVR_cI_c CCD Observations and Analyses of the 0.9-day Period, Totally Eclipsing, Solar Type Binary, NS Camelopardalis

Ronald G. Samec
Faculty Research Associate, Pisgah Astronomical Research Institute, 1 PARI Drive, Rosman, NC 28772; ronaldsamec@gmail.com

Heather Chamberlain
Pisgah Astronomical Research Institute, 1 PARI Drive, Rosman, NC 28772; 4hcham@gmail.com

Daniel Caton
Davis Gentry
Riley Waddell
Dark Sky Observatory, Physics and Astronomy Department, Appalachian State University, 525 Rivers Street, Boone, NC 28608-2106; catondb@appstate.edu

Danny Faulkner
Johnson Observatory, 1414 Bur Oak Court, Hebron, KY 41048; dfaulkner@answersingenesis.org

Received May 15, 2020; revised June 6, July 21, 2020; Accepted July 30, 2020

Abstract CCD, BVR_cI_c light curves of NS Cam were taken on 2020 January 01, 20, 21, 22, 23, February 04, 22, 23, March 01, and April 07 at the Dark Sky Observatory, North Carolina, with the 0.81-m reflector of Appalachian State University by Daniel Caton, Danny Faulkner, and Ronald Samec. Five times of minimum light were determined from our present observations, which include three primary eclipse and two secondary eclipses. We selected four times of low light from parabola fits of ASAS-SN observations. The results include a newly determined quadratic ephemeris. Thus, from our 20.3-year study, the period is found to be decreasing. Since the estimated temperatures are ~6250 ± 500 K for the primary component and ~5690 K for the secondary component, this is probably due to magnetic braking. A Wilson-Devinney analysis reveals that the system is a W UMa shallow contact binary. The component temperature difference is ~560 K. The mass ratio is also somewhat extreme, $M_2/M_1 = 0.2130 \pm 0.0001$. The total eclipses make this a firm determination. Its Roche Lobe fill-out is 17%. The cool spot was at midlatitude (co-latititude = 45°), but overlaps the pole with a large radius of ~60° and a T-factor of ~0.68. The binary inclination is high, 85.0, resulting in total eclipses. As a result, the primary minimum has a time of constant light with an eclipse duration of 104 minutes.

1. History and observations

The initial study (light curves, classification, ephemeris, etc.) of NS Cam (NSV 3771, GSC 4373- 0708) was given by Khruslov (2006) of the SKYdot team. They classified it as an EB system with a maximum V magnitude of 12.9 and minima of 13.5 and 13.2 for the primary and secondary eclipses, respectively. The period was 0.90733 d. A number of publications have times of minimum light: Hübscher *et al.* (2012); Hübscher (2011); Hübscher and Monninger (2011). NS Cam appeared in "The 79th Name-List of Variable Stars" (Kazarovets *et al.* 2008). The system was observed by the All Sky Automated Survey as ASASSN-V J075539.65+741511.3 (Pojmański 2002), AAVSO Photometric All Sky Survey (APASS) DR9 (Henden *et al.*, 2015). ASASSN give a $V_{mean} = 12.78$, an amplitude of 0.51, and EW designation, J–K = 0.289, B–V = 0.4, E(B–V) = 0.032. Figure 1 shows the ASAS light curves.

The ASASSN ephemeris is:

$$\text{HJD (MinI)} = 2458026.13575 + 0.907311\,\text{d} \times \text{E} \qquad (1)$$

From the ASAS-SN curves we were able to phase the data with Equation 1 and do parabola fits to the primary and secondary minima to locate two times of "low light" within 0.001 phase of each. This system was observed as a part of our professional collaborative studies of interacting binaries at Pisgah Astronomical Research Institute from data taken from DSO observations. The observations were taken by D. Caton, R. Samec, and D. Faulkner.. Reduction and analyses were done by R. Samec. CCD, Johnson-Cousins B, V, R_c, I_c light curves of NS Cam were taken on 2020 January 01, 20, 21, 22, 23; 2020 February 04, 22, 23; 2020 March 01; and 2020 April 07 at the

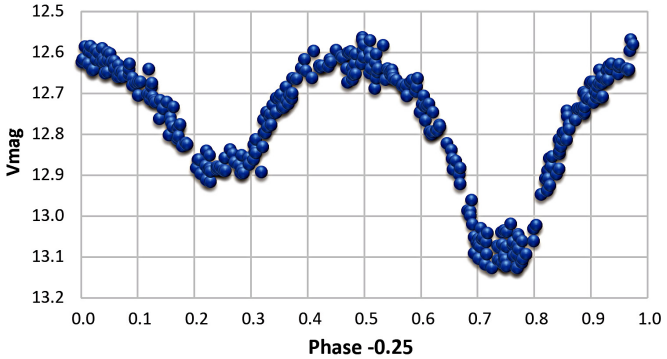

Figure 1. ASASSN-V J075539.65+741511.3 light curves (Kochanek *et al.* 2008; Shapee *et al.* 2014). Note the secondary eclipse shows a possible time of constant light (eg., a total eclipse) (Kohanek 2017).

Table 1. Sample of first ten NS Cam B, V, R_c, I_c observations.

ΔB	HJD 2458800+	ΔV	HJD 2458800+	ΔR	HJD 2458800+	ΔI	HJD 2458800+
–1.552	69.4809	–1.085	69.4814	–0.829	71.4788	–0.540	71.4791
–1.509	69.4825	–1.059	69.4830	–0.817	71.4804	–0.518	71.4807
–1.479	69.4841	–1.054	69.4846	–0.801	71.4820	–0.505	71.4823
–1.479	69.4857	–1.033	69.4862	–0.757	71.4876	–0.453	71.4879
–1.434	69.4889	–1.024	69.4893	–0.743	71.4892	–0.441	71.4895
–1.446	69.4905	–0.988	69.4910	–0.719	71.4908	–0.426	71.4911
–1.412	69.4921	–0.960	69.4926	–0.687	71.4952	–0.396	71.4955
–1.398	69.4937	–0.967	69.4942	–0.689	71.4968	–0.396	71.4971
–1.370	69.4986	–0.942	69.4990	–0.688	71.4984	-0.391	71.4987
–1.386	69.5002	–0.936	69.5007	–0.687	71.5020	-0.403	71.5023

Note: First ten data points of NS Cam B, V, R_c, I_c observations.
The full table is available through the AAVSO ftp site at ftp://ftp.aavso.org/public/datasets/samec482-nscam.txt (if necessary, copy and paste link into the address bar of a web browser).

Table 2. Photometric targets.

Star	Name	R.A. (2000) h m s	Dec. (2000)[1] ° ′ ″	V	J–K
V (Variable)	NS Cam GSC 4373-0708 NSV 3771 NSVS 685415 NSVS 767639 NSVS 685415 NSVS 738923 AN 213.1937 2MASS J05185809+3658060 HV 74374	07 55 39.62	+74 15 11.31	11.73	0.289±0.038
C (Comparison)	GSC 4373-0859 3UC329-031308	07 54 38.87	+74 14 20.81	12.99	0.28
K (Check)	GSC 4373-0770 3UC329-031303	07 54 33.18	+74 14 49.41	13.08	0.72

[1] *UCAC3 is the USNO CCD Astrograph Catalog (Zacharias* et al. *2010)*

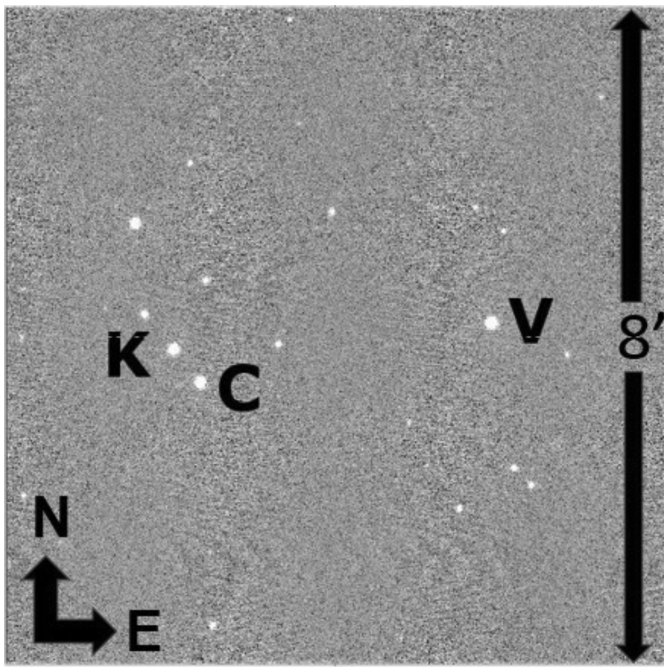

Figure 2. Finder chart, NS Cam (V), Comparison star (C), and check (K).

Dark Sky Observatory, North Carolina, with the 0.81-m reflector of Appalachian State University.

Individual observations included 923 in B, 922 in V, 917 in R_c, and 861 in I_c. The standard error of a single observation was 1.3% in B and V and 1.5% in R_c, and I_c. The nightly C–K values stayed fairly constant throughout the observing run with a precision of about 2%. Exposure times varied, from 50 s in B, 30 s in V, and 20 s in R_c and I_c. To produce these images, nightly images were calibrated with 25 bias frames, at least five flat frames in each filter, and ten 300-second dark frames. The observations are given in Table 1. Our photometric targets are designated V (variable), C (comparison), and check (K) and are given in Table 2. The variable's distance is 1,325 (56) pc (Gaia DR2 1135341864164077568). A finding chart of the field is given as Figure 2. B, V, and B–V nightly light curves of 2020 February 04 and 2020 January 01 are given in Figures 3 and 4, respectively.

2. Period determination

Five mean times (from B, V, R_c, I_c data) of minimum light were calculated from our present observations, three primary and two secondary eclipses:

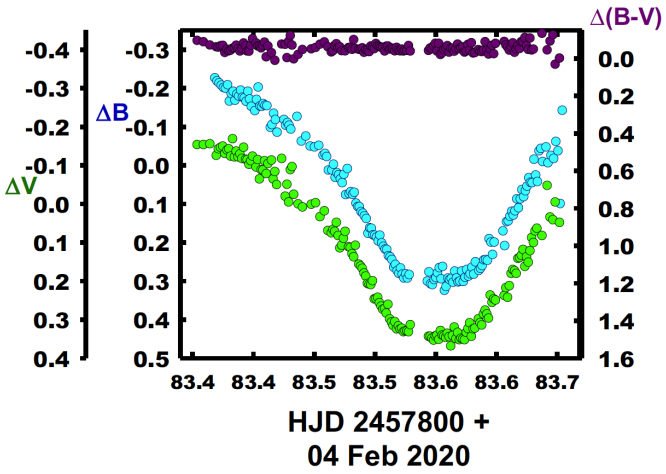

Figure 3. B, V light curves, B–V color curves from 2020 February 04.

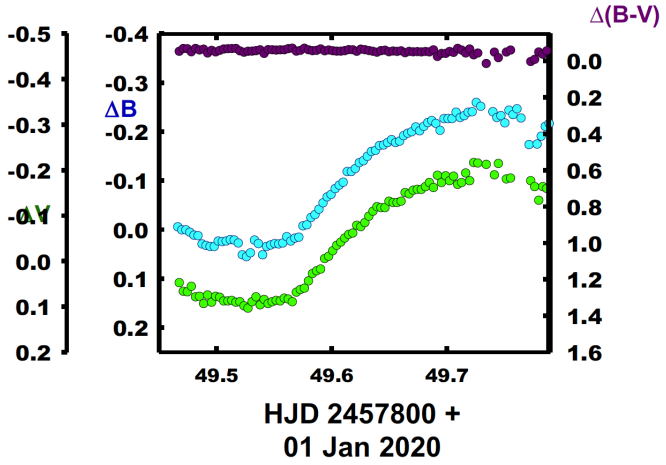

Figure 4. B, V light curves, B–V color curves from 2020 January 01.

$$\begin{aligned}\text{HJD (MinI)} &= 2458870.84278 \pm 0.00160,\\ &\quad 2458883.54736 \pm 0.00068,\\ &\quad 2458909.8621 \pm 0.0019\end{aligned}$$

(The second of the timings above was used as the initial epoch in the calculation for displayed in Table 3. The initial period was 0.907311d (ASASSN value).)

$$\begin{aligned}\text{HJD (MinII)} &= 2458849.5230 \pm 0.0011,\\ &\quad 2458946.6110 \pm 0.0006\end{aligned}$$

These minima were weighted as 1.0 in the period study. In addition, four times of low light were calculated from the ASAS-SN data and were weighted 0.1. From AAVSO's Bob Nelson's Binary O–C files (Nelson 2014) we obtained two minima from the BAVM 225. From these timings, ephemerides have been calculated, a linear and a quadratic one:

$$\begin{aligned}\text{HJD (MinI)} &= 2457883.6854 \pm 0.0005\\ &\quad + 0.90731683 \pm 0.00000017 \times E \qquad (2)\end{aligned}$$

$$\begin{aligned}\text{HJD (MinI)} &= 2458883.54853 \pm 0.00052\\ &\quad + 0.90731541 \pm 0.00000000040\\ &\quad - 0.00000000020 \pm 0.00000000005 \times E^2 \qquad (3)\end{aligned}$$

The results of the quadratic period study are displayed in Figure 5. The linear and quadratic residuals are shown in Table 3. We note here that our period study with only eleven times of minimum light (less the ASAS-SN times of low light) still gives a very similar quadratic term result –0.00000000019 ± 0.00000000006.

The quadratic ephemeris yields (although tentative) a $\dot{P} = -2.25 \times 10^{-7}$ d / yr or a mass exchange rate of

$$\frac{dM}{dt} = \frac{\dot{P} M_1 M_2}{3P (M_1 - M_2)} = \frac{-2.72 \times 10^{-8} M_\odot}{d}. \qquad (4)$$

in a conservative scenario (the primary component is the gainer). The phased B, V, R_c, and I_c light curves and B–V and R_c–I_c color curves are displayed in Figures 6 and 7, respectively, with Equation 2 used to phase the data.

3. Light curve characteristics

The curves are of good accuracy, averaging better than 1% photometric precision. Averages of the light curves at phase quadratures are given and important differences follow in Table 4. The primary amplitude of the light curve varies from 0.49 to 0.56 mag, I_c to B. The secondary amplitude was 0.28–0.29 mag. The O'Connell effect (Max I – Max II), a possible indicator of spot activity, averages about 0.015 mag. The differences in the two minima are 0.2–0.28 mag, I_c to B. A time of constant light occurs at our secondary minima and lasts some 104 minutes.

4. Temperature

The 2MASS J–K = 0.289 ± 0.038 for the binary star. This value corresponds to ~F8V ± 2, which yields a temperature of 6250 ± 500 K (Pecaut and Mamajek 2013). Fast rotating binary stars of this type are noted for having strong magnetic activity, so the binary is of solar-type with a convective atmosphere.

5. Light curve solution

The B, V, R_c, and I_c curves were pre-modeled with BINARY MAKER 3.0 (Bradstreet and Steelman 2002). Fits were determined in all filter bands, which were very stable. The solution was that of a shallow contact eclipsing binary. The parameters were then averaged (q = 0.215, fill-out = 0.08, i = 78.25, T_2 = 5650, with one cool spot) and input into a 4-color simultaneous light curve calculation using the Wilson-Devinney Program (Wilson and Devinney 1971; Wilson 1990, 1994, 2008, 2012; Van Hamme and Wilson 2007, 1998; Wilson *et al.* 2010; Wilson and Van Hamme 2014). Convective parameters g = 0.32, A = 0.5 were used. The computation was done in Mode 3 and converged to a solution. The spot turned out to be the major obstacle in computing the solution. (I first tried Mode 2 solution to determine the configuration, with the spot on the primary component. But the resulting configuration was nonphysical: The system was detached with a large spot tending to near zero or negative temperature (K). Also, the system had much the same mass ratio as our contact model.

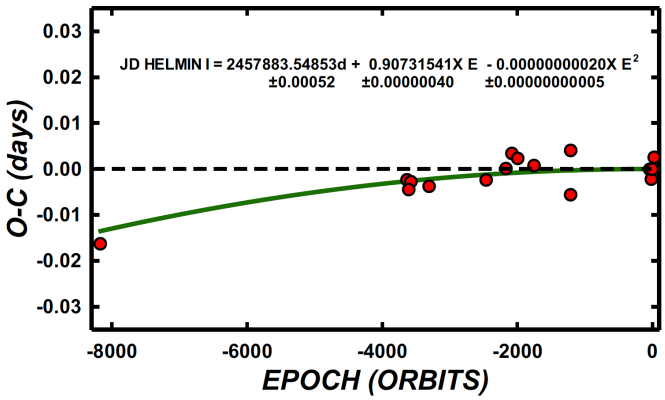

Figure 5. The linear residuals from quadratic equation (Equation 2) overlaying a plot of the quadratic term versus the orbital epoch in the period study of NS Cam.

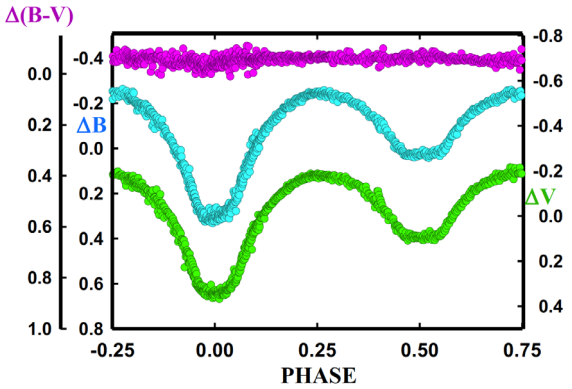

Figure 6. The phased B and V light curves and B–V color curve for NS Cam.

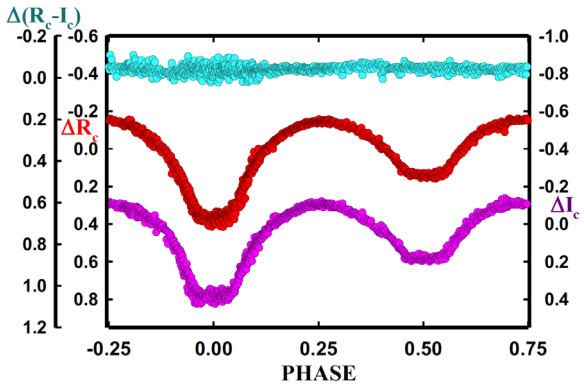

Figure 7. The phased R_c and I_c light curves and R_c–I_c color curve for NS Cam.

The separate components, if single and main sequence, would have a component temperature difference of about 3000 K. But the modeled component temperature difference was only 535 K. This would be very improbable. By switching the spot to the secondary component, the system converged to a contact solution with a reasonable spot temperature. This is very possible for a poor thermal contact system.) The spot was eventually found to be on the smaller component facing away from the primary component. We tried third light but that did not solve any fitting issues. The solution follows in Table 4. B, V, R_c, I_c normalized fluxes and B–V and R_c–I_c color curves overlaid by our solution curves of NS Cam are given in Figures 8 and 9. The geometrical representations are shown at quadratures in Figure 10a–d. The residuals of the light curves are shown in Figure 11. The fill-out of the binary is

$$f = \frac{\Omega_1 - \Omega_{ph}}{\Omega_1 - \Omega_2} = \frac{2.264754 - 2.2418}{2.264754 - 2.129279} = 0.17 \qquad (5)$$

where Ω_1 is the inner potential and Ω_2 is the outer potential.

6. Discussion

NS Cam is an eclipsing binary star with solar type components and a 0.9-day period. Since the eclipses were total, the mass ratio, q, is well determined (Terrell and Wilson 2005) with a fill-out of 17 ± 1%. The system has a fairly extreme mass ratio of ~0.21, and a component temperature difference of 560 K, which is consistent with a system in shallow contact. One major spot was needed in the final modeling. The cool spot (t-fact = 0.68) (The temperature of (Solar) sunspots have an umbral t-fact of 3800 K / 5800 K = 0.66 so our T-Fact is not strange, especially for fast rotating binary stars.) was facing away from the primary component with a colatitude of 45° and a large radius of 60°. The spot does include the pole of the secondary component. Spots of this size are better described as a spotted region, that is, it is probably made up of many spots in that region. The inclination of ~85° resulted in a time of constant light in the secondary eclipse. Its photometric spectral type indicates a primary surface temperature of ~6250 K and a secondary component temperature of ~5684 K, making it a solar type binary. Using Kepler's Law, mass ratio, M_1 = 1.18 $M_\odot$, and the orbital period, we obtain a semimajor axis, $a = a_1 + a_2 = 4.446\ R_\odot$. In terms of the solar radii, the dimensions of the system are given in Table 5.

7. Conclusion

A single 6250 K main-sequence single star would have a mass of 1.21 $M_\odot$. The mass ratio of 0.213 would mean the secondary component mass of 0.26 $M_\odot$. Such a main sequence star would have a temperature of 3250 K (M3.5V), which gives a component temperature difference of 3000 K! However, the actual value is only ~560 K. Thus, the secondary temperature is heavily influenced by the primary component, which makes the contact mode the only physical possibility. In the 23-year period study, the weak but steady decrease in the O–C curve may be due to the continuous magnetic braking. The longer, 0.9-day period (as compared to many W UMa binaries) results in a subdued but prevailing magnetic braking. Thus, the system will likely eventually coalesce into a single, fast rotating ~F4V star after a cataclysmic Red Novae event (Tylenda and Kamiński 2016).

8. Future work

Radial velocities would be highly desirable to obtain absolute (not relative) system parameters. Further light curves and eclipse timings will go toward affirming or disaffirming period scenario given here.

Table 3. Quadratic and linear residuals from NS Cam period study.

	Epoch 2400000+	*Cycle*	*Initial Residual*	*Linear Residual*	*Quadratic Residual*	*Weight*	*Error*	*Reference*
1	51473.4900	–8167.0	–0.0484	–0.0027	0.0000	1.0	—	Khruslov (2006)
2	55591.3528	–3628.5	–0.0166	0.0026	0.0009	1.0	0.0063	Hübscher (2011)
3	55644.4303	–3570.0	–0.0168	0.0021	0.0004	1.0	0.0076	Hübscher *et al.* (2012)
4	55614.4872	–3603.0	–0.0186	0.0005	–0.0013	0.5	vis	Hübscher and Lehman (2012)
5	55887.5897	–3302.0	–0.0167	0.0006	–0.0011	0.5	vis	Hübscher and Lehman (2012)
6	56654.2722	–2457.0	–0.0120	0.0004	–0.0011	0.5	0.0101	Hübscher (2014)
7	56920.1180	–2164.0	–0.0084	0.0023	0.0010	0.1	—	ASAS–SN (Shappee *et al.* 2014; Kochanek *et al.* 2017)
8	56999.9650	–2076.0	–0.0047	0.0055	0.0041	0.1	—	ASAS–SN (Shappee *et al.* 2014; Kochanek *et al.* 2017)
9	57787.9590	–1207.5	–0.0103	–0.0052	–0.0059	0.1	—	ASAS–SN (Shappee *et al.* 2014; Kochanek *et al.* 2017)
10	57788.8760	–1206.5	–0.0006	0.0045	0.0038	0.1	—	ASAS–SN (Shappee *et al.* 2014; Kochanek *et al.* 2017)
11	57077.9930	–1990.0	–0.0055	0.0042	0.0029	0.1	—	ASAS–SN (Shappee *et al.* 2014; Kochanek *et al.* 2017)
12	57297.1080	–1748.5	–0.0061	0.0022	0.0011	0.1	—	ASAS–SN (Shappee *et al.* 2014; Kochanek *et al.* 2017)
13	58849.5230	–37.5	–0.0002	–0.0019	–0.0012	1.0	0.0011	This paper
14	58870.8428	–14.0	–0.0022	–0.0041	–0.0033	1.0	0.0016	This paper
15	58883.5474	0.0	0.0000	–0.0019	–0.0012	1.0	0.0007	This paper
16	58909.8621	29.0	0.0027	0.0006	0.0014	1.0	0.0019	This paper
17	58946.6110	69.5	0.0055	0.0032	0.0041	1.0	0.0006	This paper
		r.m.s.	0.00315	0.00267				

Table 4. Light curve characteristics of NS Cam.

Filter	*Phase 0.00*	*Magnitude ± σ Min. I*	*Phase 0.25*	*Magnitude ± σ Max. I*
B		0.301 ± 0.018		–0.243 ± 0.006
V		0.345 ± 0.010		–0.179 ± 0.006
R		0.375 ± 0.020		–0.144 ± 0.006
I		0.370 ± 0.120		–0.103 ± 0.008
Filter	*Phase 0.50*	*Magnitude ± σ Min. I*	*Phase 0.75*	*Magnitude ± σ Max. I*
B		0.024 ± 0.004		–0.259 ± 0.014
V		0.092 ± 0.092		–0.198 ± 0.022
R		0.136 ± 0.007		–0.153 ± 0.005
I		0.174 ± 0.009		–0.118 ± 0.019

Filter	*Min. I – Max. II ± σ*	*Max. I – Max. II ± σ*	*Min. I – Min. II ± σ*
B	0.560 ± 0.032	0.016 ± 0.018	0.277 ± 0.021
V	0.543 ± 0.032	0.019 ± 0.042	0.253 ± 0.102
R	0.528 ± 0.025	0.009 ± 0.008	0.239 ± 0.026
I	0.487 ± 0.139	0.015 ± 0.002	0.196 ± 0.129

Filter	*Min. II – Max. II ± σ*	*Min. II – Max. I ± σ*
B	0.283 ± 0.018	0.268 ± 0.010
V	0.290 ± 0.114	0.271 ± 0.098
R	0.289 ± 0.012	0.280 ± 0.013
I	0.292 ± 0.028	0.277 ± 0.017

Table 5. B, V, Rc, Ic Wilson-Devinney program solution parameters for NS Cam.

Parameters	*Values of Contact Solution*
λB, λV, λR, λI (nm)	440, 550, 640, 790
$g_1 = g_2$	0.32
$A_1 = A_2$	0.5
Inclination (°)	85.0 ± 0.1
T_1, T_2 (K)	6250, 5689 ± 3
Ω	2.2418 ± 0.0005
$q(m_2/m_1)$	0.2130 ± 0.0002
Fill-outs: $F_1 = F_2$ (%)	17 ± 1
$L_1/(L_1+L_2)_I$	0.8422 ± 0.0005
$L_1/(L_1+L_2)_R$	0.8494 ± 0.0004
$L_1/(L_1+L_2)_V$	0.8577 ± 0.0004
$L_1/(L_1+L_2)_B$	0.8750 ± 0.0004
JDo (days)	2458883.5476 ± 0.0001
Period (days)	0.907393 ± 0.000004
R_1/a, R_2/a (pole)	0.4877 ± 0.0008, 0.2430 ± 0.0013
R_1/a, R_2/a (side)	0.5312 ± 0.0006, 0.2536 ± 0.0015
R_1/a, R_2/a (back)	0.5559 ± 0.0009, 0.2914 ± 0.0031
Spot I, Star 2	
Colatitude (°)	44.6 ± 0.2
Longitude (°)	177.4 ± 0.3
Radius (°)	59.7 ± 0.3
T-Factor (Tspot/Tsurface)	0.679 ± 0.03

Table 6. NS Cam system dimensions.

R1, R2 (pole, $R_\odot$)	2.1683 ± 0.0036	1.0804 ± 0.0089
R1, R2 (side, $R_\odot$)	2.4591 ± 0.0044	1.1271 ± 0.0107
R1, R2 (back, $R_\odot$)	2.4782 ± 0.0058	1.2951 ± 0.0213

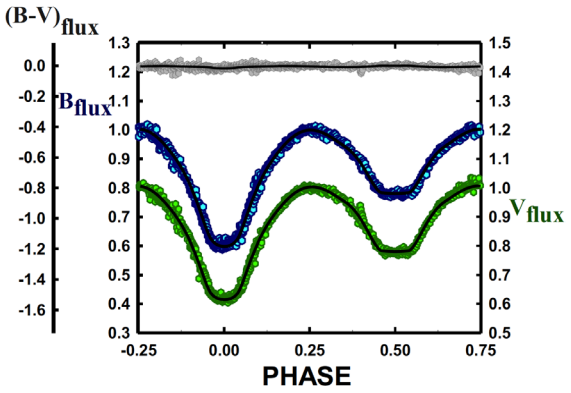

Figure 8. B and V normalized fluxes and B–V color curve overlaid by our solution curves of NS Cam.

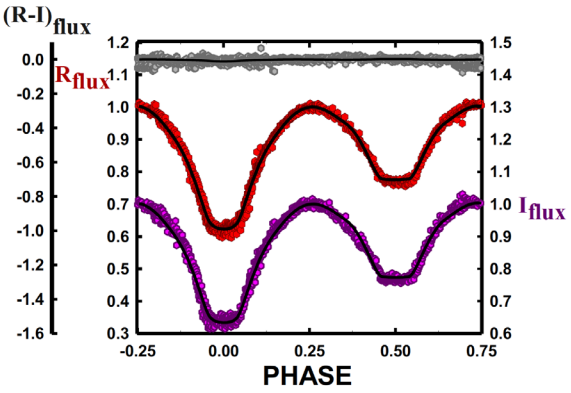

Figure 9. R_c and I_c normalized fluxes and R–I color curve overlaid by our solution curves of NS Cam.

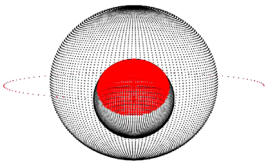

Figure 10a. NS Cam, geometrical representation at phase 0.0, with spot.

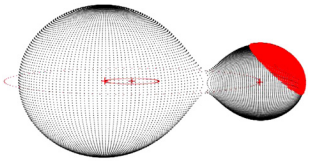

Figure 10b. NS Cam, geometrical representation at phase 0.25, with spot.

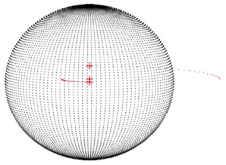

Figure 10c. NS Cam, geometrical representation at phase 0.50, with spot.

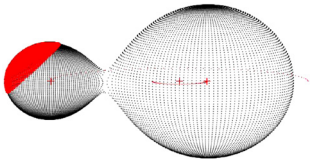

Figure 10d. NS Cam, geometrical representation at phase 0.75, with spot.

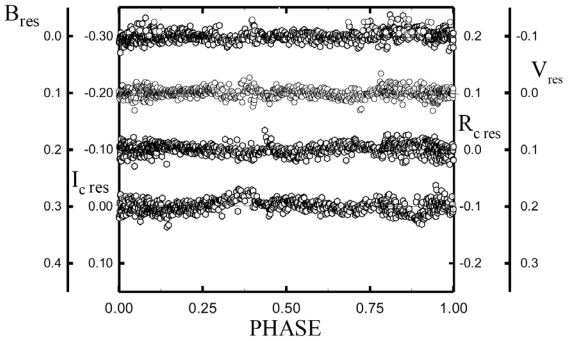

Figure 11. Residuals of the B, V, R_c, and I_c light curve solutionss.

References

Bradstreet, D. H., and Steelman, D. P. 2002, *Bull. Amer. Astron. Soc.*, **34**, 1224.

Henden, A. A., Levine, S., Terrell, D., and Welch, D. L. 2015, Amer. Astron. Soc., AAS Meeting #225, id.336.16.

Hübscher, J. 2011, *Inf. Bull. Var. Stars*, No. 5984, 1.

Hübscher, J. 2014, *Inf. Bull. Var. Stars*, No. 6118, 1.

Hübscher, J., and Lehmann, P. B. 2012, *Inf. Bull. Var. Stars*, No. 6026, 1.

Hübscher, J., Lehmann, P. B., and Walter, F. 2012, *Inf. Bull. Var. Stars*, No. 6010, 1.

Hübscher, J., and Monninger, G. 2011, *Inf. Bull. Var. Stars*, No. 5959, 1.

Kazarovets, E. V., Samus, N. N., Durlevich, O. V., Kireeva, N. N., and Pastukhova, E. N. 2008, *Inf. Bull. Var. Stars*, No. 5863, 1.

Kochanek, C. S., *et al.*, G. 2017, *Publ. Astron. Soc. Pacific*, **129**, 104502.

Khruslov, A.V. 2006, *Inf. Bull. Var. Stars*, No. 5699, 9.

Nelson, R. 2014, AAVSO O–C database (http://www.aavso.org/bob-nelsons-o-c-files).

Pecaut, M. J., and Mamajek, E. E. 2013, *Astrophys. J., Suppl. Ser.*, **208**, 9 (https://www.pas.rochester.edu/~emamajek/EEM_dwarf_UBVIJHK_colors_Teff.txt).

Pojmański, G. 2002, *Acta Astron.*, **52**, 397.

Shappee, B. J., *et al.* 2014, *Astrophys. J.*, **788**, 48.

Terrell, D., and Wilson, R. E. 2005, *Astrophys. Space Sci.*, **296**, 221.

Tylenda, R., and Kamiński, T. 2016, *Astron. Astrophys.*, **592A**, 134.

Van Hamme, W., and Wilson, R. E. 2007, *Astrophys J.*, **661**, 1129.

Van Hamme, W. V., and Wilson, R. E. 1998, *Bull. Amer. Astron. Soc.*, **30**, 1402.

Wilson, R. E. 1990, *Astrophys. J.*, **356**, 613.

Wilson, R. E. 1994, *Publ. Astron. Soc. Pacific*, **106**, 921.

Wilson, R. E. 2008, *Astrophys. J.*, **672**, 575.

Wilson, R. E. 2012, *Astron. J.*, **144**, 73.

Wilson, R. E., and Devinney, E. J. 1971, *Astrophys. J.*, **166**, 605.

Wilson, R. E., and Van Hamme, W. 2014, *Astrophys. J.*, **780**, 151.

Wilson, R. E., Van Hamme, W., and Terrell, D. 2010, *Astrophys. J.*, **723**, 1469.

Zacharias, N., *et al.* 2010, *Astron. J.*, **139**, 2184.